Inorg. Chem. **2006**, *45*, 5291–5301

Speciation of the Curium(III) Ion in Aqueous Solution: A Combined Study by Quantum Chemistry and Molecular Dynamics Simulation

Tianxiao Yang[†] and Bruce E. Bursten*[,†,‡]

Department of Chemistry, The Ohio State University, Columbus, Ohio 43210, and Department of Chemistry, University of Tennessee, Knoxville, Tennessee 37996

Received August 12, 2005

The structures of aquo complexes of the curium(III) ion have been systematically studied using quantum chemical and molecular dynamics (MD) methods. The first hydration shell of the Cm^{3+} ion has been calculated using density functional theory (DFT), with and without inclusion of the conductor-like polarizable continuum medium (CPCM) model of solvation. The calculated results indicate that the primary hydration number of Cm^{3+} is nine, with a Cm–O bond distance of 2.47–2.48 Å. The calculated bond distances and the hydration number are in excellent agreement with available experimental data. The inclusion of a complete second hydration shell of Cm^{3+} has been investigated using both DFT and MD methods. The presence of the second hydration shell has significant effects on the primary coordination sphere, suggesting that the explicit inclusion of second-shell effects is important for understanding the nature of the first shell. The calculated results indicate that 21 water molecules can be coordinated in the second hydration shell of the Cm^{3+} ion. MD simulations within the hydrated-ion model suggest that the second-shell water molecules exchange with the bulk solvent with a lifetime of 161 ps.

1. Introduction

The behavior of actinide ions in water is intensely relevant to current issues involving actinide waste storage, remediation, potential transport through various water supplies, and actinide separation technology. It is also an intensely complex thermodynamic and kinetic problem because of the high pH dependence of the species in solution, the dynamics between the coordinated water molecules and the bulk solvent, and the coordination flexibility of actinide ions. Complexes of ions of the early actinides with water have been of considerable experimental[1−18] and theoretical[18−31] interest. In this paper we will focus on speciation of the Cm^{3+} ion, which is in the middle of the actinide series and provides a bridge between the prevalent early actinides and the more difficult

* To whom correspondence should be addressed. E-Mail: bbursten@utk.edu. Phone: (865) 974-4377. Fax: (865) 974-4352.
† The Ohio State University.
‡ University of Tennessee.

(1) Bardin, N.; Rubini, P.; Madic, C. *Radiochim. Acta* **1998**, *83*, 189.
(2) Johansson, G.; Magini, M.; Ohtaki, H. *J. Solution Chem.* **1991**, *20*, 775.
(3) Moll, H.; Denecke, M. A.; Jalilehvand, F.; Sandström, M.; Grenthe, I. *Inorg. Chem.* **1999**, *38*, 1795.
(4) Sandström, M.; Persson, I.; Jalilehvand, F.; Lindquist-Reis, P.; Spångberg, D.; Hermansson, K. *J. Synchrotron Radiat.* **2001**, *8*, 657.
(5) Allen, P. G.; Bucher, J. J.; Shuh, D. K.; Edelstein, N. M.; Reich, T. *Inorg. Chem.* **1997**, *36*, 4676.
(6) Allen, P. G.; Bucher, J. J.; Shuh, D. K.; Edelstein, N. M.; Craig, I. *Inorg. Chem.* **2000**, *39*, 595.
(7) Antonio, M. R.; Williams, C. W.; Soderholm, L. *Radiochim. Acta* **2002**, *90*, 851.
(8) Neuefeind, J.; Soderholm, L.; Skanthakumar, S. *J. Phys. Chem. A* **2004**, *108*, 2733.
(9) Clark, D. L.; Conradson, S. D.; Donohoe, R. J.; Keogh, D. W.; Morris, D. E.; Palmer, P. D.; Rogers, R. D.; Tait, C. D. *Inorg. Chem.* **1999**, *38*, 1456.
(10) Clark, D. L.; Conradson, S. D.; Neu, M. P.; Palmer, P. D.; Runde, W.; Tait, C. D. *J. Am. Chem. Soc.* **1997**, *119*, 5259.
(11) Clark, D. L.; Conradson, S. D.; Ekberg, S. A.; Hess, N. J.; Neu, M. P.; Palmer, P. D.; Runde, W.; Tait, C. D. *J. Am. Chem. Soc.* **1996**, *118*, 2089.
(12) Williams, C. W.; Blaudeau, J. P.; Sullivan, J. C.; Antonio, M. R.; Bursten, B. E.; Soderholm, L. *J. Am. Chem. Soc.* **2001**, *123*, 4346.
(13) Conradson, S. D.; Abney, K. D.; Begg, B. D.; Brady, E. D.; Clark, D. L.; Den Auwer, C.; Ding, M.; Dorhout, P. K.; Espinosa-Faller, F. J.; Gordon, P. L.; Haire, R. G.; Hess, N. J.; Hess, R. F.; Keogh, D. W.; Lander, G. H.; Lupinetti, A. J.; Morales, L. A.; Neu, M. P.; Palmer, P. D.; Paviet-Hartmann, P.; Reilly, S. D.; Runde, W. H.; Tait, C. D.; Veirs, D. K.; Wastin, F. *Inorg. Chem.* **2004**, *43*, 116.
(14) Conradson, S. D.; Begg, B. D.; Clark, D. L.; Den Auwer, C.; Espinosa-Faller, F. J.; Gordon, P. L.; Hess, N. J.; Hess, R.; Keogh, D. W.; Morales, L. A.; Neu, M. P.; Runde, W.; Tait, C. D.; Veirs, D. K.; Villella, P. M. *Inorg. Chem.* **2003**, *42*, 3715.
(15) Conradson, S. D.; Begg, B. D.; Clark, D. L.; den Auwer, C.; Ding, M.; Dorhout, P. K.; Espinosa-Faller, F. J.; Gordon, P. L.; Haire, R. G.; Hess, N. J.; Hess, R. F.; Keogh, D. W.; Lander, G. H.; Manara, D.; Morales, L. A.; Neu, M. P.; Paviet-Hartmann, P.; Rebizant, J.; Rondinella, V. V.; Runde, W.; Tait, C. D.; Veirs, D. K.; Villella, P. M.; Wastin, F. *J. Solid State Chem.* **2005**, *178*, 521.
(16) Kimura, T.; Kato, Y. *J. Alloys Compd.* **1998**, *271*, 867.
(17) Kimura, T.; Nagaishi, R.; Takuo, O.; Arisaka, M.; Yoshida, Z. *J. Nucl. Sci. Technol.* **2002**, *Supplement 3*, 233.

10.1021/ic0513787 CCC: $33.50
Published on Web 06/13/2006

to study later actinides. The speciation of the Cm^{3+} ion has attracted extensive experimental study,[32−35] in large part because curium is produced in nuclear power reactors and causes many of the long-term radiological and thermal problems associated with reactor waste storage and disposal.[36]

The hydration number (i.e., the preferred number of coordinated H_2O molecules) of the Cm^{3+} ion has been investigated using a number of experimental methods. On the basis of luminescence measurements, Kimura et al.[32] proposed that the hydration number of Cm^{3+} is eight or nine in various aqueous solutions. Similarly, Stumpf et al.[33] and Moll et al.[35] used time-resolved laser-fluorescence spectroscopy to conclude that Cm(III) forms nine-coordinate complexes in glycolic acid and in water. Allen et al.[6] used EXAFS spectroscopy to investigate the coordination of a variety of trivalent lanthanide and actinide ions in aqueous solution with varying chloride concentrations. They found that at low chloride concentration, the hydration number of Cm^{3+} is 10.2 and the Cm−O bond length is 2.45 Å. It is notable that there is disagreement about the experimental coordination number for the Cm^{3+} ion on the basis of different experimental methods. In these experimental studies, the number of coordinated waters in the first hydration shell has been measured, but the detailed structure of the first hydration shell has not been clearly established. To the best of our knowledge, there have been no reports concerning the coordination number and the structure of the second hydration shell of Cm^{3+}.

There has been only scant previous theoretical study of the hydration of Cm^{3+}, including most notably the all-electron Dirac−Hartree−Fock calculations on $[Cm(H_2O)_n]^{3+}$ (n = 1, 2, 4, and 6) by Mochizuki and co-workers.[37] They found, not surprisingly, that the calculated Cm−O distance increases and the stabilization energy per water molecule decreases as the coordination number increases. This study did not include coordination numbers as high as those observed experimentally. In the highest-coordination-number species investigated, namely $[Cm(H_2O)_6]^{3+}$, the calculated Cm−O bond distance is 2.41 Å.

In this contribution, we present a full theoretical investigation on the speciation of the Cm^{3+} ion in aqueous solution. First, we will explore the hydration number and static structure of the first hydration shell of Cm^{3+} using scalar-relativistic density functional theory (DFT). These calculations are carried out on isolated "gas-phase" ions as well as in models that include the influence of the bulk aqueous solvent. We believe that the inclusion of the solvent effects is indicated by several recent theoretical studies on both the geometries and energies of actinide complexes with various solvent models.[20,38,39] The rapid development of both theoretical and computational methods facilitates detailed studies of the structures and thermodynamics of actinide complexes in solution. Here, we model the solvent effects using the conductor-like polarizable continuum model (CPCM),[40] a model that has been used successfully to determine the geometries and energies in thorium(IV),[20] uranyl(VI),[38,39] and lanthanide(III)[41] systems. We will then explicitly investigate the influence of water molecules in the second hydration shell on the structure of the first hydration shell. In particular, we will show that the water molecules of the first hydration shell form strong hydrogen bonds with those in the second shell because of polarization by the highly charged Cm^{3+} cation. To consider the strong hydrogen bonds between the first and the second hydration shells, it is crucial that we optimize the structure explicitly, including the solvent molecules in the second hydration shell. There are some publications[42] that calculate the transition metal cation hydrates using the discrete model. However, the discrete model comes with a substantial increase in computational expense for the actinide system, and very few theoretical simulation results using the discrete model are reported.

(18) Bolvin, H.; Wahlgren, U.; Moll, H.; Reich, T.; Geipel, G.; Fanghaenel, T.; Grenthe, I. *J. Phys. Chem.* A **2001**, *105*, 11441.
(19) Yang, T. X.; Tsushima, S.; Suzuki, A. *J. Phys. Chem. A* **2001**, *105*, 10439.
(20) Tsushima, S.; Yang, T. X.; Mochizuki, Y.; Okamoto, Y. *Chem. Phys. Lett.* **2003**, *375*, 204.
(21) Tsushima, S.; Yang, T. X.; Suzuki, A. *Chem. Phys. Lett.* **2001**, *334*, 365.
(22) Tsushima, S.; Suzuki, A. *J. Mol. Struct. (THEOCHEM)* **2000**, *529*, 21.
(23) Spencer, S.; Gagliardi, L.; Handy, N. C.; Ioannou, A. G.; Skylaris, C. K.; Willetts, A.; Simper, A. M. *J. Phys. Chem. A* **1999**, *103*, 1831.
(24) Blaudeau, J. P.; Zygmunt, S. A.; Curtiss, L. A.; Reed, D. T.; Bursten, B. E. *Chem. Phys. Lett.* **1999**, *310*, 347.
(25) Antonio, M. R.; Soderholm, L.; Williams, C. W.; Blaudeau, J. P.; Bursten, B. E. *Radiochim. Acta* **2001**, *89*, 17.
(26) Hay, P. J.; Martin, R. L.; Schreckenbach, G. *J. Phys. Chem. A* **2000**, *104*, 6259.
(27) Clavaguera-Sarrio, C.; Brenner, V.; Hoyau, S.; Marsden, C. J.; Millie, P.; Dognon, J. P. *J. Phys. Chem. B* **2003**, *107*, 3051.
(28) Tsushima, S.; Yang, T. X. *Chem. Phys. Lett.* **2005**, *401*, 68.
(29) Semon, L.; Boehme, C.; Billard, I.; Hennig, C.; Lutzenkirchen, K.; Reich, T.; Rossberg, A.; Rossini, I.; Wipff, G. *ChemPhysChem* **2001**, *2*, 591.
(30) Moskaleva, L. V.; Kruger, S.; Sporl, A.; Rosch, N. *Inorg. Chem.* **2004**, *43*, 4080.
(31) Vallet, V.; Privalov, T.; Wahlgren, U.; Grenthe, I. *J. Am. Chem. Soc.* **2004**, *126*, 7766.
(32) (a) Kimura, T.; Nagaishi, R.; Kato, Y.; Yoshida, Z. *Radiochim. Acta* **2001**, *89*, 125. (b) Kimura, T.; Choppin, G. R.; Kato, Y.; Yoshida, Z. *Radiochim. Acta* **1996**, *72*, 61. (c) Kimura, T.; Choppin, G. R. *J. Alloys Compd.* **1994**, *213/214*, 313. (d) Kimura, T.; Kato, Y.; Takeishi, H.; Choppin, G. R. *J. Alloys Compd.* **1998**, *271*, 719. (e) Tian, G. X.; Kimura, T.; Yoshida, Z.; Zhu, Y. J.; Rao, L. F. *Radiochim. Acta* **2004**, *92*, 495.
(33) Stumpf, T.; Fanghanel, T.; Grenthe, I. *J. Chem. Soc., Dalton Trans.* **2002**, *20*, 3799.
(34) Lindqvist-Reis, P.; Menze, R.; Schubert, G.; Fanghanel, T. *J. Phys. Chem. B* **2005**, *109*, 3077.
(35) Moll, H.; Geipel, G.; Bernhard, G. *Inorg. Chim. Acta* **2005**, *358*, 2275.
(36) Katz, J. J.; Seaborg, G. T.; Morss, L. R. *The Chemistry of The Actinide Elements*, 2nd ed.; Chapman and Hall: London, 1986; Vol. 2.
(37) (a) Mochizuki, Y.; Tatewaki, H. *J. Chem. Phys.* **2002**, *116*, 8838. (b) Mochizuki, Y.; Tatewaki, H.; Okamoto, Y. *J. Nucl. Sci. Technol.* **2002**, *Supplement 3*, 418.
(38) Vallet, V.; Wahlgren, U.; Szabo, Z.; Grenthe, I. *Inorg. Chem.* **2002**, *41*, 5626.
(39) Vallet, V.; Wahlgren, U.; Schimmelpfennig, B.; Moll, H.; Szabo, Z.; Grenthe, I. *Inorg. Chem.* **2001**, *40*, 3516.
(40) Barone, V.; Cossi, M. *J. Phys. Chem. A* **1998**, *102*, 1995.
(41) Cosentino, U.; Villa, A.; Pitea, D.; Moro, G.; Barone, V. *J. Phys. Chem. B* **2000**, *104*, 8001.
(42) (a) Li, J.; Fisher, C. L.; Chen, J. L.; Bashford, D.; Noodleman, L. *Inorg. Chem.* **1996**, *35*, 4694. (b) Rudolph, W. W.; Pye, C. C.; Irmer, G. *J. Raman Spectrocs.* **2002**, *33*, 177. (c) Rudolph, W. W.; Mason, R.; Pye, C. C. *Phys. Chem. Chem. Phys.* **2000**, *2*, 5030. (d) Martinez, J. M.; Pappalardo, R. R.; Marcos, E. S.; Mennucci, B.; Tomasi, J. *J. Phys. Chem. B* **2002**, *106*, 1118.

Finally, we report the first investigation of the dynamic properties of the second hydration shell of Cm^{3+} by the hydrated-ion concept within molecular dynamics (MD) methodology. It has long been recognized that ions, especially highly charged monatomic cations, can be treated as single-entity hydrated ions $[M(H_2O)_n]^{m+}$ with respect to interaction with the bulk water. The concept of the hydrated ion can be applied only to hydrated ions of high stability; thus, the residence time of first-hydration-shell water molecules should be long compared to the MD simulation times. The residence times of tetravalent actinide complexes $[U(H_2O)_{10}]^{4+}$ and $[Th(H_2O)_{10}]^{4+}$ are reported to be $1.67-2.08 \times 10^5$ ps and 2×10^4 ps, respectively, by NMR measurement.[43] Though there are no experimental data for the residence time of the first hydration shell of the Cm(III) ion in aqueous solution, a comparison with the trivalent lanthanide complexes $[Ln(H_2O)_n]^{3+}$ ($n = 8$ and 9) is instructive. Aqua complexes of Ln^{3+} and An^{3+} of similar ionic radii are expected to have similar structures and dynamic properties.[34,44] The residence times of a water molecule in the first hydration shell of Nd^{3+}, Sm^{3+}, and Yb^{3+} were reported by MD simulations to be 1577, 170, and 410 ps, respectively.[45] EXAFS measurements[6] reported that, at low chloride concentration, 9.5 water molecules coordinate to Nd^{3+} with a Nd−O bond length of 2.49 Å and 10.2 water molecules coordinate to Cm^{3+} with a Cm−O bond length of 2.45 Å. We therefore expect that the residence time of the water molecules in the first hydration shell of Cm^{3+} should be at least the same or longer than that of Nd^{3+} ion. Therefore, the $[Cm(H_2O)_9]^{3+}$ ion can be considered stable enough to allow us to apply the concept of the hydrated ion to perform MD studies on the second hydration shell of the Cm^{3+} ion. The basic scheme of the present MD calculations is the same as in the previous study.[19]

2. Quantum Chemical Calculation of $[Cm(H_2O)_n]^{3+}$ in Aqueous Solution

2.1. Computational Details. The trivalent Cm ion has a $5f^7$ electronic configuration, which leads to an $^8S_{7/2}$ term under LS coupling. Seven open f shells can complicate quantum chemical calculations on Cm^{3+}, especially in aqueous solution, although because the half-filled shell leads to $L = 0$, spin-orbit effects can be ignored.

All DFT calculations were carried out using the Gaussian03 package.[46] The B3LYP hybrid-density functional (Becke's three parameter hybrid functional using the LYP correlation functional[47,48]) was used, as it has reproduced accurate geometries and energies for actinide coordination complexes.[39,49−52] Relativistic effective core potentials (RECP) of the Stuttgart type were used for the Cm atom, which includes 36 valence electrons and 60 core electrons.[53] The 6-311G* all-electron basis set was used for hydrogen and oxygen atoms.[54] The solvent effects were approximated using the Gaussian03 implementation of the conductor-like polarizable continuum medium (CPCM) solvent model, where the solute is embedded in a shape-adapted cavity consisting of interlocking spheres centered on each solute atom or group.

To confirm that the optimized structures are true minima, we performed vibrational frequency calculations to ensure that all force constants were real. Because the frequency calculations in solution proved very difficult, we performed gas-phase frequency analyses on aqueous-phase structures, assuming the vibrations to be identical in vacuum and in solution.[55]

The geometry optimizations are made without any symmetry constraints. Basis set superposition error (BSSE) corrections are not taken into account. As noted earlier, spin-orbit effects are not needed because the Cm^{3+} ion has an $^8S_{7/2}$ ground state. In addition, we find that the use of scalar-relativistic effects in the DFT formalism, without spin-orbit effects, generally leads to highly accurate calculated molecular geometries and vibrational frequencies for the ground-state properties of actinide complexes.[56]

2.2. Results and Discussion. We investigated the possible static structures of hydrated complexes of Cm^{3+} with 8−12 water ligands. The geometry optimizations on these complexes were performed generally without any symmetry constraints in aqueous phase at the B3LYP/6-311G* level using the CPCM method. Table 1

(43) Farkas, I.; Banyai, I.; Szabo, Z.; Wahlgren, U.; Grenthe, I. *Inorg. Chem.* **2000**, *39*, 799.
(44) David, F. H.; Fourest, B. *New J. Chem.* **1997**, *21*, 167.
(45) Kowall, T.; Foglia, F.; Helm, L.; Merbach, A. E. *Chem.—Eur. J.* **1996**, *2*, 285.
(46) Frisch, M. J.; Trucks, G. W.; Schlegel, H. B.; Scuseria, G. E.; Robb, M. A.; Cheeseman, J. R.; Montgomery, J. A., Jr.; Vreven, T.; Kudin, K. N.; Burant, J. C.; Millam, J. M.; Iyengar, S. S.; Tomasi, J.; Barone, V.; Mennucci, B.; Cossi, M.; Scalmani, G.; Rega, N.; Petersson, G. A.; Nakatsuji, H.; Hada, M.; Ehara, M.; Toyota, K.; Fukuda, R.; Hasegawa, J.; Ishida, M.; Nakajima, T.; Honda, Y.; Kitao, O.; Nakai, H.; Klene, M.; Li, X.; Knox, J. E.; Hratchian, H. P.; Cross, J. B.; Adamo, C.; Jaramillo, J.; Gomperts, R.; Stratmann, R. E.; Yazyev, O.; Austin, A. J.; Cammi, R.; Pomelli, C.; Ochterski, J. W.; Ayala, P. Y.; Morokuma, K.; Voth, G. A.; Salvador, P.; Dannenberg, J. J.; Zakrzewski, V. G.; Dapprich, S.; Daniels, A. D.; Strain, M. C.; Farkas, O.; Malick, D. K.; Rabuck, A. D.; Raghavachari, K.; Foresman, J. B.; Ortiz, J. V.; Cui, Q.; Baboul, A. G.; Clifford, S.; Cioslowski, J.; Stefanov, B. B.; Liu, G.; Liashenko, A.; Piskorz, P.; Komaromi, I.; Martin, R. L.; Fox, D. J.; Keith, T.; Al-Laham, M. A.; Peng, C. Y.; Nanayakkara, A.; Challacombe, M.; Gill, P. M. W.; Johnson, B.; Chen, W.; Wong, M. W.; Gonzalez, C.; Pople, J. A. *Gaussian 03*, revision A.1; Gaussian, Inc.: Pittsburgh, PA. (b) Frisch, M. J.; Trucks, G. W.; Schlegel, H. B.; Scuseria, G. E.; Robb, M. A.; Cheeseman, J. R.; Montgomery, Jr., J. A.; Vreven, T.; Kudin, K. N.; Burant, J. C.; Millam, J. M.; Iyengar, S. S.; Tomasi, J.; Barone, V.; Mennucci, B.; Cossi, M.; Scalmani, G.; Rega, N.; Petersson, G. A.; Nakatsuji, H.; Hada, M.; Ehara, M.; Toyota, K.; Fukuda, R.; Hasegawa, J.; Ishida, M.; Nakajima, T.; Honda, Y.; Kitao, O.; Nakai, H.; Klene, M.; Li, X.; Knox, J. E.; Hratchian, H. P.; Cross, J. B.; Adamo, C.; Jaramillo, J.; Gomperts, R.; Stratmann, R. E.; Yazyev, O.; Austin, A. J.; Cammi, R.; Pomelli, C.; Ochterski, J. W.; Ayala, P. Y.; Morokuma, K.; Voth, G. A.; Salvador, P.; Dannenberg, J. J.; Zakrzewski, V. G.; Dapprich, S.; Daniels, A. D.; Strain, M. C.; Farkas, O.; Malick, D. K.; Rabuck, A. D.; Raghavachari, K.; Foresman, J. B.; Ortiz, J. V.; Cui, Q.; Baboul, A. G.; Clifford, S.; Cioslowski, J.; Stefanov, B. B.; Liu, G.; Liashenko, A.; Piskorz, P.; Komaromi, I.; Martin, R. L.; Fox, D. J.; Keith, T.; Al-Laham, M. A.; Peng, C. Y.; Nanayakkara, A.; Challacombe, M.; Gill, P. M. W.; Johnson, B.; Chen, W.; Wong, M. W.; Gonzalez, C.; Pople, J. A. *Gaussian 03*, revision C.02; Gaussian, Inc.: Wallingford, CT, 2004.
(47) Becke, A. D. *J. Chem. Phys.* **1993**, *98*, 5648.
(48) Lee, C. T.; Yang, W. T.; Parr, R. G. *Phys. Rev. B* **1988**, *37*, 785.
(49) Schreckenbach, G.; Hay, P. J.; Martin, R. L. *J. Comput. Chem.* **1999**, *20*, 70.
(50) Schreckenbach, G.; Hay, P. J.; Martin, R. L. *Inorg. Chem.* **1998,** *37*, 4442.
(51) Clark, A. E.; Martin, R. L.; Hay, P. J.; Green, J. C.; Jantunen, K. C.; Kiplinger, J. L. *J. Phys. Chem. A* **2005**, *109*, 5481.
(52) Sonnenberg, J. L.; Hay, P. J.; Martin, R. L.; Bursten, B. E. *Inorg. Chem.* **2005**, *44*, 2255.
(53) Kuchle, W.; Dolg, M.; Stoll, H.; Preuss, H. *J. Chem. Phys.* **1994**, *100*, 7535.
(54) Krishnan, R.; Binkley, J. S.; Seeger, R.; Pople, J. A. *J. Chem. Phys.* **1980**, *72*, 650.
(55) Tomasi, J.; Persico, M. *Chem. Rev.* **1994**, *94*, 2027.
(56) Li, J.; Bursten, B. E. *Computational Organometallic Chemistry*; Cundari, T. R., Ed.; Marcel Dekker: New York, 2001; p 345.

Table 1. Optimized Geometric Parameters and Free Energies of $[Cm(H_2O)_n]^{3+}$ (n = 8, 9, 10, and 12) Complexes in Aqueous Phase from B3LYP/6-311G* DFT Calculations

CN	complex	symmetry	Cm−O (Å) (gas phase)	Cm−O_I (Å) (aqueous phase)	G (Hartree) (aqueous phase)	ΔG^a (kcal/mol) (aqueous phase)	q_{Cm}
8	$[Cm(H_2O)_8]^{3+}$	D_{2d}	2.50 × 4, 2.52 × 4	2.44 × 4, 2.45 × 4	−1250.576928	0	+2.070
	$[Cm(H_2O)_8]^{3+}$	C_s		2.42−2.48	−1250.568114	4.59	+2.082
	$[Cm(H_2O)_8]^{3+}$	D_{4d}	2.52 × 8	2.46 × 8	−1250.563274	5.74	+2.271
	$[Cm(H_2O)_8]^{3+}$	D_{4h}	2.54 × 8	2.47 × 8	−1250.546010	15.04	+2.200
9	$[Cm(H_2O)_9]^{3+}$	D_3	2.55 × 3, 2.53 × 6	2.48 × 3, 2.47 × 6	−1327.052241	0	+2.150
	$[Cm(H_2O)_9]^{3+}$	D_{3h}	2.59 × 3, 2.52 × 6	2.49 × 3, 2.47 × 6	−1327.046165	4.83	+2.165
	$[Cm(H_2O)_8(H_2O)]^{3+}$	C_1		2.43−2.45 × 8, 4.14	−1327.048093	5.12	+2.091
10	$[Cm(H_2O)_{10}]^{3+}$	D_2		2.65 × 2, 2.51 × 4, 2.52 × 4	−1403.501657	6.63	+2.078
	$[Cm(H_2O)_{10}]^{3+}$	D_{5d}	2.66 × 10	2.59 × 10	−1403.454672	31.53	+2.078
	$[Cm(H_2O)_8(H_2O)_2]^{3+}$	C_1		(2.44−2.46) × 8, 4.15 × 2	−1403.514583	0	+2.072
	$[Cm(H_2O)_9(H_2O)_1]^{3+}$	C_s		2.46−2.52, 4.02	−1403.513547	0.32	+2.001
12	$[Cm(H_2O)_8(H_2O)_4]^{3+}$	D_2		2.45 × 4, 2.45 × 4, 4.20 × 4	−1556.448575	1.51	+1.974
	$[Cm(H_2O)_9(H_2O)_3]^{3+}$	C_1		(2.48−2.51) × 9, 4.26, 4.30, 4.34	−1556.450165	0	+2.031
	$[Cm(H_2O)_{10}(H_2O)_2]^{3+}$	C_1		(2.51−2.62) × 10	−1556.437055	7.74	+1.942

[a] The zero-point energy (ZPE) corrections are included in the relative energies ΔG.

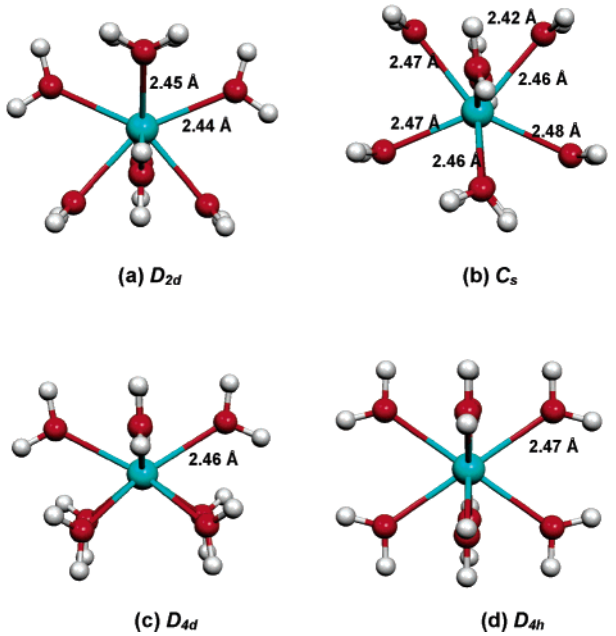

Figure 1. Optimized structures of $[Cm(H_2O)_8]^{3+}$ with (a) D_{2d}, (b) C_s, (c) D_{4d}, and (d) D_{4h} point symmetries in aqueous solution on the basis of CPCM calculations.

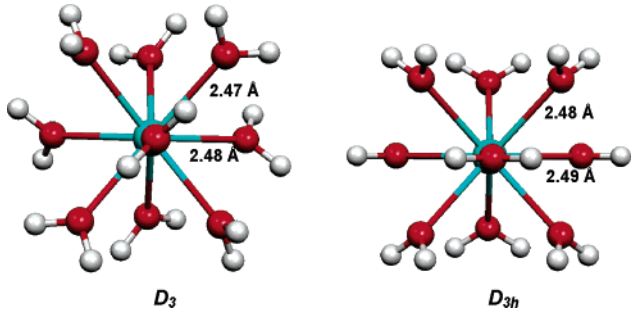

Figure 2. Optimized structures of $[Cm(H_2O)_9]^{3+}$ of D_3 and D_{3h} point symmetries in aqueous solution on the basis of CPCM calculations.

presents the calculated geometries and free energies for $[Cm(H_2O)_n]^{3+}$ (n = 8, 9, 10, and 12) in aqueous solution. The zero-point energy (ZPE) corrections are included in relative energies ΔG. For comparison, some complexes were also optimized as isolated gas-phase ions at the same theoretical level; the Cm−O bond distances are given in the same table.

$[Cm(H_2O)_8]^{3+}$. Depending on the symmetry of the CmO_8 coordination sphere and the orientation of the H atoms, the coordination of eight H_2O ligands to Cm^{3+} can lead to a variety of geometries that conform to different molecular point groups. We fully optimized possible structures for $[Cm(H_2O)_8]^{3+}$ under four different point-group symmetries, namely D_{2d}, D_{4h}, D_{4d}, and C_s. The optimized structures and energies are given in Table 1 and Figure 1. The relative total energies suggest that the D_{2d} structure that can be described as having a distorted cubic geometry is the most stable; we find it to be 4.59, 5.74, and 15.04 kcal/mol more stable than C_s, D_{4d}, and D_{4h} structures, respectively. The net atomic charge on the Cm atom, which is an indicator of the ability of the H_2O ligands to donate to the metal, is +2.07 e in D_{2d} symmetry, which is lower than that in the D_{4h}, D_{4d}, and C_s structures. The D_{2d} symmetry also exhibits the shortest Cm−O bond distances (2.44−2.45 Å), which further supports the notion that the D_{2d} structure is the optimum one for $[Cm(H_2O)_8]^{3+}$ in aqueous solution.

$[Cm(H_2O)_9]^{3+}$. For the nine-water-molecule complex, we calculated three possible structures. The first two of these have all nine H_2O ligands in the primary coordination sphere (Figure 2), namely a D_{3h} symmetry structure with a tricapped trigonal prismatic arrangement of the oxygen atoms, and a D_3 structure, also based on a tricapped trigonal prismatic geometry, in which the H atoms of the three water molecules in the equatorial plane "gear" about their C_2 axes. The third structure is a C_1 8+1 structure, in which one H_2O ligand is moved out of the first coordination shell and bonded in the second shell at a Cm−O bond distance of 4.14 Å (see Figure S1 in the Supporting Information). In the D_3 symmetry, the dihedral angle between the plane of the equatorial water and the equatorial plane is 45.8°. The Cm−O bond distance to the three equatorial oxygen atoms is 2.48 Å, 0.01 Å shorter than that in the D_{3h} structure, mainly because of the decrease in interligand interactions upon gearing. The Cm−O bond length to the six prismatic oxygen atoms is 2.47 Å, which is the same as that in the D_{3h} structure. The D_3 configuration leads to a molecular energy 4.83 kcal/mol lower than that in the D_{3h} configuration. The net atomic charge on the Cm atom of D_3 configuration is +2.150 e (Table 2), 0.015 e lower than that of the D_{3h} configuration, indicating slightly stronger O-to-Cm donation in the D_3 conformation. The 8+1 structure is 5.12 kcal/mol higher in energy than the D_3 structure, indicating that the preferred coordination number is nine at this level of calculation. All of the calculated frequencies for the D_3 structure are real; thus, this structure is a true minimum. Interestingly, Matonic et al.[57] found that in the crystal structure of

(57) Matonic, J. H.; Scott, B. L.; Neu, M. P. *Inorg. Chem.* **2001**, *40*, 2638.

Table 2. Calculated Mulliken Charges (e) of Gas-Phase $[Cm(H_2O)_9]^{3+}$ and $[Cm(H_2O)_9(H_2O)_{18}]^{3+}$ Obtained from B3LYP/6-311G* DFT Calculations

	Cm ion[a]					inner shell			outer shell		
	q_{Cm}	s	p	d	f	Σq_O	Σq_H	$\Sigma q_H - \Sigma q_O$	Σq_O	Σq_H	$\Sigma q_H - \Sigma q_O$
$[Cm(H_2O)_9]^{3+}$ (D_3)	+2.150	4.131	11.952	10.438	7.329	−8.073	+8.923	+0.850			
$[Cm(H_2O)_9]^{3+}$ (D_{3h})	+2.165	4.133	11.964	10.434	7.303	−7.995	+8.830	+0.835			
$[Cm(H_2O)_9(H_2O)_{18}]^{3+}$(structure A)	+1.768	4.183	11.971	10.540	7.535	−8.393	+8.687	+0.294	−15.477	+16.414	+0.937
$[Cm(H_2O)_9(H_2O)_{18}]^{3+}$ (structure B)	+2.129	4.149	11.968	10.337	7.417	−8.449	+8.298	−0.151	−15.630	+16.652	+1.022

[a] In these calculations, a neutral Cm atom has 36 electrons outside of the core, 26 of which ($s^4p^{12}d^{10}$) are generally not considered to be valence electrons.

plutonium(III) aquo complex $[Pu(H_2O)_9][CF_3SO_3]_3$, the equatorial water ligands rigorously lie perpendicular to the equatorial plane, which is different from the result we find for the isolated $Cm(H_2O)_9^{3+}$ ion. Similar behavior was reported by Harrowfield et al.[58] and Chatterjee et al.[59] for the crystal structures of the nonahydrates of the rare earth trifluoromethanesulfonates $[Ln(H_2O)_9][CF_3SO_3]_3$ (Ln = La, Ce, Pr, Nd, Sm, Eu, Gd, Tb, Dy, Yb, and Lu), namely that the planes of the equatorial water molecules are oriented perpendicular to the equatorial plane. For these crystal structures of $[Pu(H_2O)_9][CF_3SO_3]_3$ and $[Ln(H_2O)_9][CF_3SO_3]_3$, the metal−equatorial water bond distances, $M-O_{eq}$, are longer than the metal−prismatic water bond distances, $M-O_{pr}$. The crystallographic differences in the bond distances vary, from $\Delta = d(M-O_{eq}) - d(M-O_{pr}) = 0.098$ Å for Pu^{3+},[57] to $\Delta = 0.10-0.23$ Å for hydrated lanthanide ions.[58,59] We believe that the influence of the counteranion may affect the equatorial and prismatic bond lengths differently, which could explain why we do not see this effect in our calculations. Consistent with this notion, the variations in $Cm-O_c$ (capping O) and $Cm-O_p$ (prismatic O) bond distances are only 0.01 and 0.02 Å for the aqueous-phase-optimized D_3 and D_{3h} $[Cm(H_2O)_9]^{3+}$ structures, respectively.

$[Cm(H_2O)_{10}]^{3+}$. Four possible structures of Cm^{3+} interacting with 10 H_2O ligands were investigated. Structures of D_2 and D_{5d} symmetry in which all 10 ligands are in the first coordination shell, a 9+1 structure $[Cm(H_2O)_9(H_2O)_1]^{3+}$ of C_s symmetry, and an 8+2 structure $[Cm(H_2O)_8(H_2O)_2]^{3+}$ of C_1 symmetry. The optimized structures are given in Figure S2 of the Supporting Information. As shown in Table 1, the 8+2 structure is found to be the lowest in energy, with the 9+1 structure only 0.32 kcal/mol higher. Both the D_2 and D_{5d} structures are considerably higher in energy, allowing us to conclude that a maximum of nine water ligands will coordinate in the first shell, presumably because of steric crowding of the H_2O ligands. It is interesting to note that the calculations on the nine-water-molecule complexes suggest a preferred coordination number of nine in the first shell, whereas the 10-water-molecule calculations suggest that eight coordination is preferred, albeit by a trivial amount of energy.

We further investigated three possible 12-water-molecule complexes, namely 8+4 $[Cm(H_2O)_8(H_2O)_4]^{3+}$, 9+3 $[Cm(H_2O)_9(H_2O)_3]^{3+}$, and 10+2 $[Cm(H_2O)_{10}(H_2O)_2]^{3+}$. The optimized structures are given in Figure S3 of the Supporting Information. As shown in Table 1, we find that $[Cm(H_2O)_9(H_2O)_3]^{3+}$ is the lowest-energy structure, although it is only 1.51 kcal/mol more stable than $[Cm(H_2O)_8(H_2O)_4]^{3+}$. Thus, as in the other calculations, the structures with eight and nine H_2O ligands in the first coordination shell are very close in energy. The more sterically congested 10+2 $[Cm(H_2O)_{10}(H_2O)_2]^{3+}$ structure is 7.74 kcal/mol higher in energy than the 9+3 structure.

To summarize these calculations on the first coordination sphere, we see that $[Cm(H_2O)_9]^{3+}$ is 5.12 kcal/mol lower in energy than $[Cm(H_2O)_8(H_2O)_1]^{3+}$, $[Cm(H_2O)_8(H_2O)_2]^{3+}$ is 0.32 kcal/mol lower in energy than $[Cm(H_2O)_9(H_2O)_1]^{3+}$, and $[Cm(H_2O)_9(H_2O)_3]^{3+}$ is 1.51 kcal/mol lower in energy than $[Cm(H_2O)_8(H_2O)_4]^{3+}$. The optimized Cm−O bond distances are 2.44−2.45 Å in $[Cm(H_2O)_8]^{3+}$ (in D_{2d} symmetry) and 2.47−2.48 Å in $[Cm(H_2O)_9]^{3+}$ (in D_3 symmetry); the slightly shorter distance in the eight-coordinate system is consistent with the notion of coordinative saturation with nine ligands in the first coordination shell. The calculated Cm−O bond distances in both $[Cm(H_2O)_8]^{3+}$ and $[Cm(H_2O)_9]^{3+}$ are in good agreement with the experimental values of 2.45−2.46 Å reported by Allen et al.[6] and 2.46 Å reported by Stumpf et al.[60] Overall, our calculated geometries and energies favor a maximum of nine water ligands in the first shell, although it also seems that eight-coordination is possible. This conclusion is in good accord with the available experimental studies, which report that the coordination number of Cm^{3+} in H_2O is 8 or 9.[32−35,60]

These calculations also suggest that the use of a solvation model, such as the CPCM method, is important in modeling the Cm−O bond distances in the first coordination shell of Cm^{3+}. As noted above, the bond distances calculated with the CPCM method included are in good agreement with the experimental values. In Table 1, we also report the gas-phase (i.e., no solvation model included) results on several of the same Cm^{3+} complexes. In each case, the gas-phase calculations lead to significantly longer Cm−O bond distances. For example, gas-phase $[Cm(H_2O)_8]^{3+}$ with D_{2d} symmetry has Cm−O bond distances of 2.50−2.52 Å, a range that is 0.06−0.07 Å longer than those of the aqueous-phase structure at the same computational level. Likewise, gas-phase $[Cm(H_2O)_9]^{3+}$ with D_3 symmetry has Cm−O bond distances of 2.53−2.55 Å, 0.06−0.07 Å longer than those of the aqueous-phase structure. For these systems, it seems evident that at the same computational level, the solvent effects induce a decrease in the Cm−O bond distance by 0.06−0.07 Å. This observation demonstrates that the surrounding effects should be included in the geometry optimization to obtain molecular structures in better agreement with solution experimental structures. In the next section, we will report results in which the second hydration shell is explicitly included in the quantum chemical calculations.

2.3. The Second Hydration Shell of the Cm^{3+} Ion. The preceding section suggests that knowledge of the second-hydration-shell structure will help to understand the polarization and charge transfer between the central metal ion and the outer shell waters. There are very few publications on the structure of the second hydration shell of actinide ions. Johansson et al.[2] reported that in dilute perchlorate solution, about 20 water molecules were present in the second hydration shell of the Th^{4+} ion at a Th−O bond distance of 4.6 Å. A review paper by Rizkalla et al.[61] summarized

(58) Harrowfield, J. M.; Kepert, D. L.; Patrick, J. M.; White, A. H. *Aust. J. Chem.* **1983**, *36*, 483.
(59) Chatterjee, A.; Maslen, E. N.; Watson, K. J. *Acta Crystallogr., Sect. B* **1988**, *44*, 381.
(60) Stumpf, T.; Funke, H.; Hennig, C.; Roberg, A.; Reich, T.; Fanghnel, T. *Annual Report 2002*; Institute of Radiochemistry, Forschungszentrum Rossendorf: Dresden, Germany, 2002; p 1. See http://www.fz-rossendorf.de/FWR/DOCS/JB2002Netz.pdf.
(61) Rizkalla, E. N.; Choppin, G. R. *Handbook on the Physics and Chemistry of Rare Earths*; Gschneidner, K. A., Eyring, L., Jr., Choppen, G. R., Lander, G. H., Eds.; North-Holland Publishing: Amsterdam, 1994; Vol. 18, p 529.

Table 3. Optimized Geometric Parameters and Energies for $[Cm(H_2O)_9(H_2O)_n]^{3+}$ (n = 18, 19, 20, and 21) Complexes from B3LYP/6-311G* DFT with CPCM Solvent Corrections

	Cm−O_I (Å)	Cm−O_{II} (Å)	E (SCF) (Hartree)	CPCM[a] (kcal/mol)	ΔE (kcal/mol)
$[Cm(H_2O)_9(H_2O)_{18}]^{3+}$ (structure A)	2.52 × 9	4.80	−2702.983583	−289.90	5.22
$[Cm(H_2O)_9(H_2O)_{18}]^{3+}$ (structure B)	2.54 × 3, 2.49 × 6	4.72	−2702.980233	−297.22	0
$[Cm(H_2O)_9(H_2O)_{18}(H_2O)_2]^{3+}$	2.44−2.54		−2855.897992	−274.70	19.69
$[Cm(H_2O)_9(H_2O)_{20}]^{3+}$	2.49−2.58	4.68	−2855.894872	−296.35	0
$[Cm(H_2O)_9(H_2O)_{21}]^{3+}$	2.48−2.54	4.70	−2932.365689	−293.86	0
$[Cm(H_2O)_9(H_2O)_{18}(H_2O)_3]^{3+}$	2.50−2.53		−2932.374198	−283.96	4.56

[a] Energy stabilization due to the conductor-like polarized continuum model.

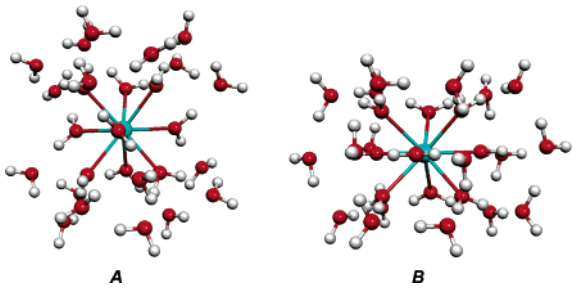

Figure 3. Optimized structures of $[Cm(H_2O)_9(H_2O)_{18}]^{3+}$. Left: structure A, for which the inner sphere $[Cm(H_2O)_9]^{3+}$ has D_3 symmetry. Right: structure B, for which the inner sphere $[Cm(H_2O)_9]^{3+}$ has D_{3h} symmetry. Under CPCM calculations, structure B is 5.22 kcal/mol more stable than structure A.

the hydration numbers and hydration radii of trivalent actinide and lanthanide ions obtained by electrophoresis and diffusion measurements. The hydration number of the second shell of the Cm^{3+} ion was reported to be 14.4 at a Cm−O bond distance of 4.69 Å. In this section, we will report theoretical calculations on the structure of the second hydration shell of the Cm^{3+} ion. In the final section, we will use MD methods to explore the exchange of water ligands between the second shell and the bulk solvent.

The approach to explicit inclusion of the second shell is analogous to that used for the first-shell calculation. We have assumed a first-shell coordination number of nine, and have explored varying numbers of water molecules in the second shell. All of these $[Cm(H_2O)_9(H_2O)_m]^{3+}$ structures have been optimized within DFT.

$[Cm(H_2O)_9(H_2O)_{18}]^{3+}$. As a starting point for models of the second hydration shell, we will consider the case that two water molecules in the second shell are hydrogen bonded to each first-shell water molecule, i.e., $[Cm(H_2O)_9(H_2O)_{18}]^{3+}$. The 2:1 ratio of second-shell to first-shell water molecules has the added advantage of allowing structures with relatively high symmetry to be explored, on the basis of the previously discussed D_3 and D_{3h} structures of $[Cm(H_2O)_9]^{3+}$.

We investigated two possible symmetric arrangements of the second-shell water molecules around the inner-sphere $[Cm(H_2O)_9]^{3+}$, namely those in which the second-shell molecules lie either in the planes or perpendicular to the planes defined by first-shell molecules. On the basis of these different starting arrangements of the second-hydration-shell waters, we calculated different gas-phase conformations of $[Cm(H_2O)_9(H_2O)_{18}]^{3+}$ at the B3LYP/6-311G* level without any symmetry constraints. The optimized structures are shown in Figure 3. The solvation energies were calculated using the CPCM method on the basis of the optimized gas-phase structures. Although the surrounding effects should be included in the geometry optimization to obtain molecular structures in better agreement with solution experimental structures, the energetics of these systems can be appropriately calculated using the gas-phase optimized structures because the term due to the geometry relaxation in solution is not significant.

When 18 waters are added to the second hydration shell of D_3 $[Cm(H_2O)_9]^{3+}$ (Figure 2), the minimum-energy structure of $[Cm(H_2O)_9(H_2O)_{18}]^{3+}$ (structure A, Figure 3) corresponds to a 3+6+6+3 arrangement of the oxygen atoms of the second hydration shell. The optimized structure and calculated energies are given in Figure 3 and Table 3. This optimized structure of $[Cm(H_2O)_9(H_2O)_{18}]^{3+}$ has approximate D_3 symmetry. The six second-shell water molecules bonded to the three first-shell equatorial water molecules have a Cm−O_{II} (i.e., Cm to second-shell oxygen atom) bond distance of 4.84 Å, whereas the 12 second-shell waters bonded to the six prismatic waters have a Cm−O_{II} distance of 4.78 Å. The average Cm−O_{II} distance is 4.80 Å. The inner sphere of $[Cm(H_2O)_9]^{3+}$ has Cm−O_I bond distances of 2.519 Å (equatorial water ligands) and 2.518 Å (prismatic water ligands).

A somewhat different result is obtained when 18 water molecules are added to D_{3h} $[Cm(H_2O)_9]^{3+}$, in which the three equatorial water ligands lie rigorously in the equatorial plane (Figure 2). The resulting minimum-energy structure of $[Cm(H_2O)_9(H_2O)_{18}]^{3+}$ (structure B, Figure 3) has approximate D_3 symmetry and corresponds to a 6+6+6 arrangement of the oxygen atoms of the second-hydration-shell water molecules. The six water molecules bonded to the three equatorial water ligands are perpendicular to the equatorial plane. In each of the sets of six second-shell water molecules, there are three at a slightly shorter distance and three at a slightly longer distance. The calculated Cm−O_{II} bond distances are 4.58(×6), 4.63(×6), and 4.97(×6) Å, leading to an average Cm−O_{II} bond distance of 4.72 Å. The inner-sphere Cm−O_I bond distances are 2.54 Å (equatorial) and 2.49 Å (prismatic). At the gas-phase level, structure A has a slightly lower energy than structure B. However, the differential stabilization of structure B upon inclusion of the CPCM method leads us to predict that structure B is 5.22 kcal/mol more stable than structure A. The optimized structure A and structure B both have real vibrational frequencies and thus correspond to local minima. To test whether the high-symmetry structure B was indeed a local minimum under a reasonable reduction of symmetry, we rotated the three first-shell equatorial waters about their C_2 axes to a point at which the dihedral angle between the equatorial water ligands and the equatorial plane is 10°. Upon optimization of this starting structure, the three equatorial water molecules indeed returned to the equatorial plane, corresponding to the D_{3h} structure of the first shell.

Recall that the overall donation from the water ligands to the Cm^{3+} ion was greater for the D_3 structure of $[Cm(H_2O)_9]^{3+}$ than for the D_{3h} structure. Population analysis indicates that this trend continues in the $[Cm(H_2O)_9(H_2O)_{18}]^{3+}$ structures. The total Mulliken populations of the 5f and 6d orbitals of structure A are 0.12 and 0.20 e larger, respectively, than those of structure B. Thus, upon inclusion of the 18 second-shell water molecules, the D_3 arrangement of the first-shell water molecules facilitates greater ligand-to-metal donation than does the D_{3h} arrangement.

The greater ligand-to-metal donation in structure A of $[Cm(H_2O)_9(H_2O)_{18}]^{3+}$ relative to structure B suggests that the former

is preferable to the latter. Indeed, as mentioned preciously, the gas-phase SCF energies in Table 3 indicate that structure A is lower in energy than structure B. However, this ordering reverses upon inclusion of the CPCM effects: structure B is differentially stabilized by 7.32 kcal/mol relative to structure A in the presence of modeled solvent. It is this solvent stabilization that causes structure B to be 5.22 kcal/mol more stable than structure A. We believe that differences in the polarization of the hydration shells leads to this energetic reversal upon solvent inclusion. In particular, the trends in the overall charges of the hydration shells, listed in Table 2, add insight to this observation. The overall charge on the inner shells of structures A and B are +0.294 and −0.151, respectively. The negative charge on the inner shell of structure B is a consequence of two effects. First, because the water molecules in the first hydration shell of structure B are less-effective donors to the Cm^{3+} ion, more charge is left on the inner-shell water molecules in structure B. This effect is underscored by the greater Mulliken charge on the Cm atom in structure B (+2.129) than in structure A (+1.768). Second, the second-shell water molecules are closer to the Cm center in structure B than in structure A (Table 3) and are therefore more-effective charge donors to the first-shell ligands. As a consequence, the total Mulliken charge of the second-shell water molecules is more positive in structure B (+1.022) than in structure A (+0.937). The greater positive charge in the second shell of structure B facilitates greater attractive interactions with the polarized continuum; in essence, these results suggest that structure B could engage in stronger hydrogen bonding with the bulk solvent than structure A, thus leading to greater differential stabilization of structure B by the solvent.

To explore even higher coordination numbers in the second shell, we added two or three additional water molecules in the equatorial plane of the second hydration shell of structure B. The optimized structure shows that the H atoms of the three equatorial water molecules of the first hydration shell gear about their C_2 axes. This observation suggests that 18 water molecules in the second shell are not adequate to model the second hydration shell completely.

$[Cm(H_2O)_9(H_2O)_{20}]^{3+}$ and $[Cm(H_2O)_9(H_2O)_{21}]^{3+}$. As noted above, the use of 18 water molecules in the second shell was a convenient starting point for the second-shell calculations because of the intrinsic symmetry that could be preserved. Nevertheless, we were not certain whether 18 was the maximum number of water molecules that could occupy the second shell. We therefore have calculated the geometries of $[Cm(H_2O)_9(H_2O)_{20}]^{3+}$ and $[Cm(H_2O)_9(H_2O)_{21}]^{3+}$ in which an additional two and three water molecules, respectively, were either placed in the second shell or allowed to occupy a new third shell at a longer Cm−O distance. The structures of these ions were first optimized at the Hartree−Fock level and then re-optimized using DFT. The solvation energies were calculated using the CPCM method. On the basis of the optimized structure of $[Cm(H_2O)_9(H_2O)_{18}]^{3+}$ (both structures A and B), we put two and three extra waters in the second hydration shell above the prismatic water planes or in the equatorial plane. When two extra waters are above the prismatic water planes, the optimization "pushes" the water molecules out of the second hydration shell. The structures in which the two and three extra water molecules lie perpendicular to the equatorial plane are also unstable. However, with appropriate initial orientation of the additional water molecules, we could obtain optimized structures in which 20 and 21 water molecules were in the second hydration shell. The optimized structures of $[Cm(H_2O)_9(H_2O)_{20}]^{3+}$ and $[Cm(H_2O)_9(H_2O)_{21}]^{3+}$ are given in Figure 4. All of the optimizations were carried out without any symmetry constraints, and the final structures typically have only C_1 point symmetry. Upon the inclusion of the additional

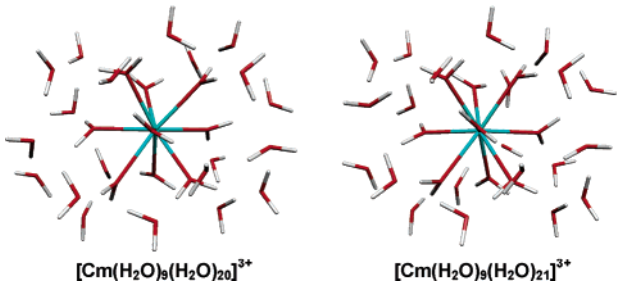

Figure 4. Optimized structures of $[Cm(H_2O)_9(H_2O)_{20}]^{3+}$ and $[Cm(H_2O)_9(H_2O)_{21}]^{3+}$.

second-shell ligands, the inner-sphere $[Cm(H_2O)_9]^{3+}$ also has only C_1 symmetry. The optimized structures reported here have all real vibrational frequencies.

The optimized structure of $[Cm(H_2O)_9(H_2O)_{20}]^{3+}$ has an average $Cm-O_{II}$ bond length of 4.68 Å. This distance is actually shorter than either of the arrangements of $[Cm(H_2O)_9(H_2O)_{18}]^{3+}$, probably as a consequence of the overall decrease in symmetry. We also optimized the 9+18+2 structure, namely 18 waters being in the second hydration shell and 2 waters being in the third shell (see Figure S4 of the Supporting Information). The energies of the optimized structures are given in Table 3. It shows that the 9+20 structure is 19.69 kcal/mol more stable than the 9+18+2 structure with the inclusion of the CPCM corrections.

Similar results are obtained when three water molecules are added to $[Cm(H_2O)_9(H_2O)_{18}]^{3+}$. The optimized structure of $[Cm(H_2O)_9(H_2O)_{21}]^{3+}$ leads to an average $Cm-O_{II}$ bond distance of 4.70 Å. The inner sphere has $Cm-O_I$ bond distances of 2.48−2.54 Å. We also optimized the 9+18+3 structure in which 18 water molecules are in the second hydration shell and three in the third shell. The calculated energies with the CPCM corrections demonstrate that the 9+21 structure is 4.56 kcal/mol more stable than the 9+18+3 structure.

The calculated energies and optimized structures of the 9+20 and 9+21 arrangements suggest that up to 21 water molecules can be coordinated in the second hydration shell. It also suggests the possibility that even more water molecules should be included in the second hydration shell. Our attempts to optimize structures with 22 or more water molecules in the second shell have been unsuccessful, perhaps indicating that 21 second-shell water molecules is the maximum number allowed in a static structure of $[Cm(H_2O)_9(H_2O)_m]^{3+}$. To compare the relative stabilities of 20 and 21 water molecules in the second shell, we also attempted calculations on a 9+20+1 structure, which would allow a direct energetic comparison to the 9+21 structure. Unfortunately, the calculations on the 9+20+1 structure did not converge.

Recall that the optimized Cm−O distance in $[Cm(H_2O)_9]^{3+}$ shortened significantly upon inclusion of the CPCM method (Table 1). Apparently, the explicit inclusion of second-shell water molecules mimics this effect to some extent. The gas-phase calculations in which the second shell is included leads to $Cm-O_I$ bond distances that are 0.04−0.05 Å shorter than those for gas-phase $[Cm(H_2O)_9]^{3+}$ in D_3 and D_{3h} symmetries (see Tables 1 and 3). However, the optimized gas-phase geometries of $[Cm(H_2O)_9(H_2O)_{18}]^{3+}$ and $[Cm(H_2O)_9(H_2O)_{21}]^{3+}$ give $Cm-O_I$ bond distances that are longer than those in CPCM-optimized $[Cm(H_2O)_9]^{3+}$. This observation suggests that the conclusions about the $[Cm(H_2O)_9(H_2O)_m]^{3+}$ systems might change somewhat if the geometries were optimized using the CPCM method explicitly rather than using a correction term. However, we are currently unable to optimize the structures of these second-shell actinide complexes in the aqueous

phase. We believe that the conclusions presented on the basis of CPCM corrections probably capture the greatest portion of the bulk solvent effects.

3. Molecular Dynamics Calculation of $[Cm(H_2O)_9]^{3+}$ in Aqueous Solution

3.1. Computational Details. The accuracy of molecular-dynamics simulation depends on the interaction potentials used to describe the forces acting among the components of the model system. One of the most usual approaches to describe the particle interactions is pairwise additivity.[62,63] However, as pointed out in the previous section, the highly charged Cm^{3+} ion produces strong interactions with and charge transfer from the outer-shell water molecules in aqueous solution. These long-distance interactions will cause the pairwise additivity model to fail because of the neglect of the nonadditive behavior of the classical electric polarization.

The hydrated-ion concept can overcome the difficulties of the electric polarization and the charge transfer.[64] The hydrated-ion model was developed in several stages. The hydrated-ion approach was first introduced by Pappalardo and co-worker[64] on the basis of the development of potentials built on the basis of ab initio interaction energies. The authors performed MD simulation and found that the hydration energies of Zn^{2+} obtained from the hydrated-ion approach are much closer to the experimental estimation than the results obtained with the potential for the single Zn^{2+} ion. The water molecules in the first hydration shell were completely rigid. Afterward, Bleuzen et al.[65] proposed the fitting of potentials using density functional calculations to reproduce experimental values of the ionic aqueous solution. The hydrogen atoms of each water molecule were allowed to rotate freely around the water dipole axis. The authors found that the simulated second coordination shell around the Cr^{3+} ion in aqueous solution structurally and dynamically compares well with the experimental measurement. Furthermore, Wasserman et al.[66] and Martinez et al.[67] developed the flexible hydrated-ion model. The hydrated-ion concept has been used successfully to study the second-hydration-shell properties of Th(IV).[9,68] Martinez et al.[67,69] and Bleuzen et al.[65] have successfully used this model to develop ab initio hydrated ion−water potentials for the small and highly charged cations Be^{2+}, Mg^{2+}, Al^{3+}, Cr^{3+}, Zn^{2+}, and Rh^{3+}. Here, we have implemented the hydrated-ion concept for Cm^{3+} by treating $[Cm(H_2O)_9]^{3+}$ as the cationic entity interacting in solution. Thus, the $Cm^{3+}-H_2O$ interaction is replaced by the hydrated ion $[Cm(H_2O)_9]^{3+}-H_2O$ interaction. The population analysis on $[Cm(H_2O)_9(H_2O)_{18}]^{3+}$ in the previous section shows that the average atomic charges on the O and H atoms in the second hydration shell are −0.868 and +0.462 e, respectively, which are close to the O and H atomic charges of −0.834 and +0.417 e in the TIP3P water model.[70] We therefore believe that we can simulate the second hydration shell and the bulk waters using the TIP3P water model. The TIP3P water model has successfully been used for MD calculations for the uranyl ion and trivalent lanthanide ions by Chaumont et al.[71] and QM/MM calculation for the uranyl system by Infante et al.[72] Kim[73] compared the Gibbs free energy and the first-hydration-shell structures of Eu^{3+} and Nd^{3+} ions using different (TIP3P, TIP4P, and SPC/E) solvent models. The author found that these three different solvent models gave the same metal−oxygen bond distance and coordination number.

The calculations were performed with the program package AMBER 7.0.[74] The interaction potentials are of pair potential type and consist of a coulomb part and Lennard−Jones (LJ) part (eq 1)

$$E(r) = q_i q_j/r - 2\epsilon(R^*/r)^6 + \epsilon(R^*/r)^{12} \quad (1)$$

The LJ parameters R^* and ϵ are the van der Waals radius and the potential well depth of the minimum energy point, respectively; q is the atomic charge.

The atomic charges of $[Cm(H_2O)_9]^{3+}$ were calculated using the ESP (electrostatic potential) method.[75] The simulation model consists of one $[Cm(H_2O)_9{}^{3+}]$ complex immersed in a periodic box of 650 water molecules together with 3 Cl^- counterions. The Cl^- ions are fully dissociated pairs in which the initial distance between the Cl^- anions and central Cm is 9 Å (approximately the cutoff distance). The Particle Mesh Ewald (PME) method is applied to calculate the long-ranged coulombic electrostatic interactions.[76]

The MD simulation was performed at 298 K starting with random velocities. The temperature was monitored by coupling the system to a thermal bath by using the Berendsen algorithm[77] with a relaxation time of 0.1 ps.

The second-shell water molecules and the bulk waters are described using the rigid TIP3P water model, and the solvent bonds were constrained with SHAKE. During the simulation, oxygen atoms are kept fixed and the hydrogen atoms rotate. LJ parameters of Cm^{3+} and the hydrogens (R^*_{Cm}, R^*_{H1}, ϵ_{Cm}, ϵ_{H_1}) are initially set to zero. First, the LJ parameters of the first-shell oxygen atoms are changed, R^*_O in the range of 1.8−2.0 Å and ϵ_{O_1} in the range of 0.042−0.060 kcal/mol, to perform MD simulations for 200 ps. We found that the LJ parameters R^*_O =1.95 Å and ϵ_{O_1} = 0.06 kcal/mol led to the bond distances $Cm-O_{II}$ = 4.65 Å, H_I-O_{II} = 1.75 Å, and O_I-O_{II} = 2.65 Å and that the second-shell coordination number is 21.0. All of these parameters are in good accord with the previous quantum chemical calculations. In addition, the bond distance of O_I-O_{II} = 2.65 Å is very close to the experimentally estimated distance of O_I-O_{II} = 2.60 Å.[78] Therefore, R^*_O = 1.95 Å and ϵ_{O_1} = 0.06 kcal/mol are used to perform the following MD simulations.

(62) Tongraar, A.; Sagarik, K.; Rode, B. M. *Phys. Chem. Chem. Phys.* **2002**, *4*, 628.
(63) Rowley, R. L.; Pakkanen, T. *J. Chem. Phys.* **1999**, *110*, 3368.
(64) Pappalardo, R. R.; Marcos, E. S. *J. Phys. Chem.* **1993**, 97, 4500.
(65) Bleuzen, A.; Foglia, F.; Furet, E.; Helm, L.; Merbach, A. E.; Weber, J. *J. Am. Chem. Soc.* **1996**, *118*, 12777.
(66) Wasserman, E.; Rustad, J. R.; Xantheas, S. S. *J. Chem. Phys.* **1997**, *106*, 9769.
(67) Martinez, J. M.; Pappalardo, R. R.; Marcos, E. S. *J. Chem. Phys.* **1998**, *109*, 1445.
(68) Yang, T. X.; Tsushima, S.; Suzuki, A. *Chem. Phys. Lett*. **2002**, 360, 534.
(69) (a) Martínez, J. M.; Hernández-Cobos, J.; Saint-Martin, H.; Pappalardo, R. R.; Ortega-Blake, I.; Marcos, E. S. *J. Chem. Phys.* **2000**, *112*, 2339. (b) Pappalardo, R. R.; Martínez, J. M.; Marcos, E. S. *J. Phys. Chem*. **1996**, *100*, 11748. (c) Martínez, J. M.; Pappalardo, R. R.; Marcos, E. S. *J. Phys. Chem. B* **1998,** *102*, 3272. (d) Martínez, J. M.; Pappalardo, R. R.; Marcos, E. S. *J. Am. Chem. Soc.* **1999**, *121*, 3175. (e) Martínez, J. M.; Pappalardo, R. R.; Marcos, E. S. *J. Chem. Phys.* **1999**, *110*, 1669. (f) Martinez, J. M.; Merkling, P. J.; Pappalardo, R. R.; Refson, K.; Marcos, E. S. *Theor. Chem. Acc*. **2004**, *111*, 101.
(70) Jorgensen, W. L.; Chandrasekhar, J.; Madura, J. D.; Impey, R. W.; Klein, M. L. *J. Chem. Phys.* **1983**, *79*, 926.
(71) Chaumont, A.; Wipff, G. *Inorg. Chem*. **2004**, *43*, 5891.
(72) Infante, I.; Visscher, L. *J. Comput. Chem*. **2004**, *25*, 386.
(73) Kim, H. S. *Chem. Phys.* **2001**, *269*, 295.
(74) Case, D. A.; Pearlman, D. A.; Caldwell, J. W.; Cheatham, T. E., III; Wang, J.; Ross, W. S.; Simmerling, C. L.; Darden, T. A.; Merz, K. M.; Stanton, R. V.; Cheng, A. L.; Vincent, J. J.; Crowley, M.; Tsui, V.; Gohlke, H.; Radmer, R. J.; Duan, Y.; Pitera, J.; Massova, I.; Seibel, G. L.; Singh, U. C.; Weiner P. K.; Kollman, P. A. *AMBER 7;* University of California: San Francisco, 2002.
(75) Besler, B. H.; Merz, K. M.; Kollman, P. A. *J. Comput. Chem.* **1990**, *11*, 431.
(76) Essmann, U.; Perera, L.; Berkowitz, M. L.; Darden, T.; Lee, H.; Pedersen, L. G. *J. Chem. Phys.* **1995**, *103*, 8577.
(77) Berendsen, H. J. C.; Postma, J. P. M.; Vangunsteren, W. F.; Dinola, A.; Haak, J. R. *J. Chem. Phys.* **1984**, *81*, 3684.

Table 4. Molecular Dynamics Simulation Conditions and Parameters for $[Cm(H_2O)_9]^{3+}$

no. of $[Cm(H_2O)_9]^{3+}$	1
no. of TIP3P water molecules	650
no. of Cl^- ions	3
box size ($Å^3$)	31 × 31 × 31
cutoff distance (Å)	10
time step (fs)	1
simulation time (ps)	1500
T (K)	298
pressure (atm)	1
Cm concentration (M)	0.058
q_{Cm}	+2.76
$q_{O_I}{}^a$ (e)	−1.08 × 6, −1.04 × 3
$q_{H_I}{}^a$ (e)	+0.55 × 12, +0.54 × 6

[a] The oxygen and hydrogen atomic charges for the three equatorial water molecules are −1.04 and +0.54 e, respectively. The oxygen and hydrogen atomic charges for the six prismatic water molecules are −1.08 and +0.55 e, respectively.

The solvated system first runs 1000 steps of energy minimization, then runs a simulation with position restraints (the NTR option of AMBER) to the solute ($[Cm(H_2O)_9{}^{3+}]$) for the initial water and counterions full equilibration around the solute. The system was equilibrated to a final temperature of 298 K in the NVE ensemble for 200 ps. The system equilibrium was checked by equilibrium density and temperature. After equilibration, the MD simulation was performed in the NPT ensemble at the expected temperature of 298 K and at constant pressure $P = 1$ atm for 1500 ps. The MD calculation used periodic boundary conditions with a time step of 1 fs. By checking the equilibration of temperature and energies (both kinetic energy and potential energy), the temperature and energies become conservative and stable after 100 ps. The cutoff distance for nonbonded interactions is 10 Å. The MD trajectories were saved every 0.1 ps. The simulation conditions are listed in Table 4.

3.2. Results and Discussion. Radial Structure of the Second Hydration Shell. One of the most experimentally relevant aspects of the MD calculations is the ability to determine radial distribution functions (RDFs) within a dynamic complex. These calculated values should be directly comparable to data obtained in EXAFS and X-ray scattering experiments of actinide ions in solution. The calculated curium−oxygen and curium−hydrogen RDFs $g(r)$ are given in Figure 5. The peaks at 4.65 Å for the oxygen and 5.25 Å for the hydrogen correspond to the second coordination sphere, which is well-defined. The broad peaks at 6.75 Å for oxygen and 7.45 Å for hydrogen correspond to the third coordination sphere, which, not surprisingly, is less well-defined. Spherical integration of $g(r)$ for oxygen between 3.00 Å and the first minimum at 5.25 Å (shown as the red line in Figure 5) shows that the mean number of water molecules in the second coordination sphere of Cm^{3+} is 21.0. During the MD simulation period of 1500 ps, no Cl^- anions were observed to enter the second coordination shell. The O_I-O_{II} distance between oxygen atoms of the first and second shell waters is 2.65 Å. The H_I-O_{II} distance between the hydrogen atom of the first-hydration-shell waters and the oxygen atom of the second hydration shell waters is 1.75 Å. The summarized MD calculated results are shown in Table 5.

Residence Time in the Second Hydration Shell. The residence time of a water molecule in the hydration shell gives deeper specific insight into the ionic hydration and the ionic mobility. The residence time is determined on the basis of the definition of $n_{ion}(t)$, which measures the number of molecules that are in a given region around

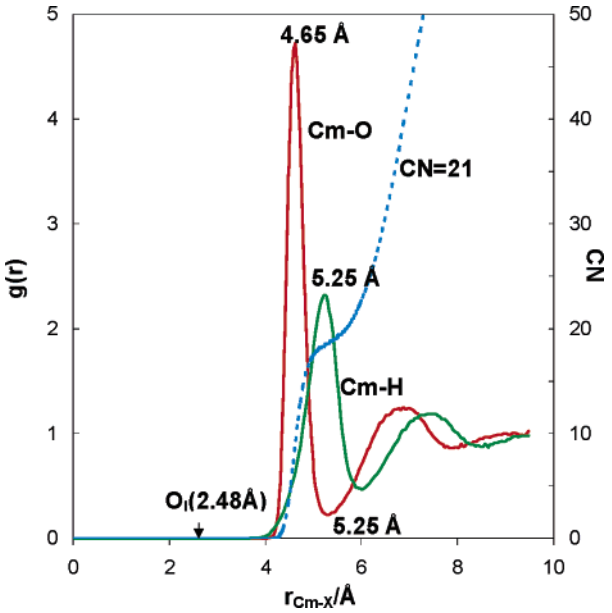

Figure 5. Cm−O and Cm−H pairs radial-distribution functions (RDFs) and the corresponding coordination number (CN) around $[Cm(H_2O)_9]^{3+}$.

Table 5. Summary of the Structural and Dynamic Results after 1500 ps MD Simulation in a Periodic Box

system	$[Cm(H_2O)_9]^{3+} + 650H_2O + 3Cl^-$
box size ($Å^3$)	27 × 27 × 27
$r_{Cm-O_{II}}$ (Å)	4.65
$r_{Cm-H_{II}}$ (Å)	5.25
$r_{O_I-O_{II}}$ (Å)	2.65
$r_{H_I-O_{II}}$ (Å)	1.75
density (g/cm^3)	1.01
H_2O coordination number	21
$g(r)_{min}$ (Å)	5.25
τ_{res} (ps)	161
T (K)	298
D^a ($cm^2\,s^{-1}$)	1.84×10^{-6}
D^b ($cm^2 s^{-1}$)	4.00×10^{-5}

[a] The self-diffusion coefficient of $[Cm(H_2O)_9]^{3+}$. [b] The self-diffusion coefficient of bulk water molecules.

the ion after a period of time t. From this definition, $n_{ion}(0)$ is the coordination numbers of the water molecules in a given region. If this region is the first hydration shell, $n_{ion}(0)$ represents the dynamic hydration number of the first shell. In our present simulation system, $n_{ion}(0)$ is the dynamic hydration number of the second shell. Excluding an initial period during which the function decays rapidly, $n_{ion}(t)$ adopts an exponential form, i.e., $n_{ion}(t) \approx e^{-t/\tau}$, where τ is a correlation time for the persistence of water molecules in a given region around the ion. The mean lifetime of a water molecule in the second coordination sphere, τ_{res}, was calculated using the formula of Impey et al.[79]

$$n_{ion}(t) = \frac{1}{N_t}\sum_{n=1}^{N_t}\sum_j P_j(t_n,t;t^*) \qquad (2)$$

$P_j(t_n,t;t^*)$ is a function that can take only a value of 1 if water molecule j lies within the region considered at both time steps t_n and $t + t_n$ not leaving the region for a period longer than t^*; otherwise, $P_j(t_n,t;t^*)$ takes a value of 0. In our calculation, we set t^* to be 2 ps. We calculated the residence probability $p(t)$ of a water molecule at a distance of $r_{Cm-O_{II}} \leq 5.25$ Å, a distance that

(78) Bergstrom, P. A.; Lindgren, J.; Read, M.; Sandstrom, M. *J. Phys. Chem.* **1991**, *95*, 7650.

(79) Impey, R. W.; Madden, P. A.; McDonald, I. R. *J. Phys. Chem.* **1983**, *87*, 5071.

corresponds to the minimum of $g(r)$ after the peak due to the second-shell oxygen atoms (Figure 5). From a least-squares fit of the calculated data to the exponential equation, we find the residence time τ_{res} to be 161 ps (see Figure S5 of the Supporting Information).

The mean lifetimes of a water molecule in the first coordination sphere of 3+ ions are experimentally found to vary over 19 orders of magnitude.[80] By comparison, knowledge of the residence time of the second coordination sphere is scarce. The residence time of water molecules in the second hydration shell for a Co^{3+} ion in aqueous solution was reported to be 55 ps from the QM/MM molecular dynamics simulation.[81] The hydrated Nd^{3+}, Sm^{3+}, and Yb^{3+} ions were reported to have residence times of 13, 12, and 18 ps, respectively, in the second hydration shell by MD calculations.[82] NMR measurements obtained a value of 128 ps for the second hydration shell of the hydrated Cr^{3+} ion.[65] Given these comparative values, we believe that the calculated value of $\tau_{res} = 161$ ps for the second-shell water molecules around Cm^{3+} indicates that the second hydration shell is stable. To date, experimental data for the residence time of the water ligands about a Cm^{3+} ion has not been reported, but our results suggest that the lifetime is long enough to allow measurements to be made.

Dynamic Properties. We believe that MD approaches will ultimately provide important information about the dynamics of actinide ions in solution and about the exchange of ion-influenced solvent molecules with the bulk. As a test of the efficacy of our MD approach, we wanted to use our results to calculate an experimentally determined property within the framework of this simulation prior to making predictions about the Cm^{3+} system. The translational self-diffusion coefficient D is a key (and extremely sensitive) property in determining the mobility of particles in solution. The diffusion coefficient D was calculated from the Einstein equation over 1500 ps

$$6Dt = \Delta r^2(t) \tag{3}$$

where $\Delta r^2(t) = \langle [r_i(t) - r_i(0)]^2 \rangle$ is the mean square displacement.

By analyzing the trajectories and calculating the mean square displacement of $[Cm(H_2O)_9]^{3+}$ and all the TIP3P water molecules, we found that the $[Cm(H_2O)_9]^{3+}$ translational self-diffusion coefficient, D, from our MD simulations is 1.84×10^{-6} cm^2 s^{-1} (Table 5). The diffusion coefficient of bulk water molecules was calculated to be 4.00×10^{-5} cm^2 s^{-1}, which compares reasonably with the diffusion coefficient of 2.89×10^{-5} cm^2 s^{-1} for pure water.[83] Unfortunately, there are no available experimental data for the diffusion coefficient of $[Cm(H_2O)_9]^{3+}$. The $[Cr(H_2O)_6]^{3+}$ diffusion coefficient was experimentally reported[84] to be 5.3×10^{-6} cm^2 s^{-1} and theoretically reported[65] by MD simulation to be 5.9×10^{-6} cm^2 s^{-1}. Given these comparative values, we believe that these results give us confidence in using the results of our MD simulations in predicting the dynamics of exchange between the water molecules surrounding the hydrated ion and those in the bulk.

Under the assumption that there are 21 water molecules in the second hydration shell, the residence time of 161 ps corresponds to 195 water exchanges in the period of 1500 ps. The water-exchange events between the second hydration shell and the bulk water observed are gathered in Figure S6 of the Supporting Information. The results of our simulation show that the crossing point between the trajectories of the incoming and outgoing water molecules is not midway between the first and second hydration shell; rather, the crossing point is displaced toward the inner shell (see Figure S6 of the Supporting Information), which supports an associative water-exchange mechanism between the second hydration shell and bulk water.

Finally, we note that our present MD simulation model assumes that the hydrate is rigid during the simulations, although the hydrogen atoms have rotational freedom. To explore the dynamic properties between the first and second hydration shells, we will need a fully flexible hydrated-ion model.

In our future work, we plan to extend this study with the introduction of complexing agents such as acetate, glycine, or glycolate. The concentration effects of the supporting electrolyte on the hydrated Cm(III) structures will also be investigated.

4. Conclusions

The combined quantum chemistry and molecular dynamics results presented here represent the first attempts to model the static and dynamic behavior of the second hydration shell of Cm^{3+}. The quantum chemistry computations performed on the Cm^{3+} ion demonstrate that in order to obtain molecular structures in better agreement with the solution experimental structures, we need to include the surrounding effects in the geometry optimizations. The relativistic density functional theory calculations on hydrated Cm(III) ion using the conductor-like polarizable dielectric continuum model (CPCM) have led to a predicted hydration number and structural parameters that are in excellent agreement with the available experimental data. The primary hydration number of the Cm^{3+} ion is 9 and the Cm−O bond length is 2.47−2.48 Å.

We have also presented the first full quantum mechanical calculation of the structure of the second hydration shell about an actinide ion. The calculated results indicate that there is strong charge transfer between the Cm^{3+} ion and the outer water molecules as well as between the first- and second-hydration-shell water molecules. The water molecules in the first hydration shell form strong hydrogen bonds with the water molecules in the second shell because of the strong polarization of the highly charged Cm^{3+} ion. The quantum chemical calculations lead us to predict that 21 waters are present in the second hydration shell of Cm^{3+}, a result that is remarkably consistent with the MD results. The MD simulations based on the rigid hydrated-ion concept give a mean lifetime of a water molecule in the second coordination sphere of 161 ps, which indicates that the second hydration shell is stable.

As noted earlier, the choice of Cm^{3+} was made for reasons of relevance and practicality—the ion is one that is relevant to the understanding of actinide ion transport, and the electronic structure of the f^7 ion obviates the need to consider spin−orbit effects. In addition, X-ray scattering experiments are currently in progress at Argonne National Laboratory that should corroborate our computational studies.[85] The methodologies we have applied here will be broadly ap-

(80) Helm, L.; Merbach, A. E. *Coord. Chem. Rev.* **1999**, *187*, 151.
(81) Kritayakornupong, C.; Plankensteiner, K.; Rode, B. M. *J. Chem. Phys.* **2003,** *119*, 6068.
(82) Kowall, T.; Foglia, F.; Helm, L.; Merbach, A. E. *J. Am. Chem. Soc.* **1995**, *117*, 3790.
(83) Harris, K. R.; Woolf, L. A. *J. Chem. Soc., Faraday Trans. 1*, **1980**, *76*, 377.
(84) Easteal, A. J.; Mills, R.; Woolf, L. A. *J. Phys. Chem.* **1989**, *93*, 4968.
(85) Soderholm, L. Personal communication, 2005.

plicable to other actinide systems (albeit with the need to consider spin−orbit effects for many of the ions), and we plan to extend these studies within the actinide series.

Acknowledgment. This research was generously supported by the Basic Energy Sciences Program of the Office of Science of the Department of Energy (Grant DE-FG02-01ER15135 in the Heavy Element Chemistry Program and Grant DE-FG02-01ER15230 in the Scientific Discovery through Advanced Computing Program) and by the Ohio State Supercomputer Center via a generous grant of computer time. The authors thank Dr. Satoru Tsushima, Department of Materials, Physics, and Energy Engineering of Nagoya University, for helpful discussion and suggestions.

Supporting Information Available: Optimized structures of $[Cm(H_2O)_8(H_2O)_1]^{3+}$, $[Cm(H_2O)_{10}]^{3+}$, $[Cm(H_2O)_8(H_2O)_2]^{3+}$, $[Cm(H_2O)_9(H_2O)_1]^{3+}$, $[Cm(H_2O)_8(H_2O)_4]^{3+}$, $[Cm(H_2O)_9(H_2O)_3]^{3+}$, $[Cm(H_2O)_{10}(H_2O)_2]^{3+}$, and $[Cm(H_2O)_8(H_2O)_{18}(H_2O)_3]^{3+}$ in the aqueous solution. The residence time of a water molecule in the second hydration shell. Water exchange between the second hydration shell and the bulk water. This material is available free of charge via the Internet at http://pubs.acs.org.

IC0513787